Rock Mechanics and Rock Engineering
https://doi.org/10.1007/s00603-018-1554-6

ORIGINAL PAPER

Use of Seismic Resonance Measurements to Determine the Elastic Modulus of Freestanding Rock Masses

Jeffrey R. Moore[1] · **Paul R. Geimer**[1] · **Riley Finnegan**[1] · **Michael S. Thorne**[1]

Received: 14 March 2018 / Accepted: 12 July 2018

Abstract
Measuring the elastic modulus of in situ rock masses over scales of tens of meters remains an important challenge in experimental rock mechanics. Here we present a new approach using ambient resonance measurements of freestanding rock landforms to identify vibrational modes, which are then matched with 3D numerical models implementing bulk, globally representative material properties. The result is an experimentally determined, albeit numerically calibrated, estimate of rock mass elastic modulus. We demonstrate the approach at five natural rock arches in southern Utah, each formed in Navajo Sandstone, where we have acquired resonance data and matched experimental resonant modes using 3D numerical modal analysis. Two material properties can be varied to match experimental data: density and modulus. We hold density constant, applying measured or reference values, and solve for elastic modulus using a forward approach. The resolved modulus is representative of the global small-strain dynamic behavior, integrating rock mass heterogeneity over the scale of the feature. The technique works well for freestanding geological landforms that exhibit clear vibrational modes. Errors arise with uncertain mechanical boundary conditions or strong material anisotropy. The resolved modulus values add relevant information describing the variation of elastic properties over scales from lab samples to in situ rock masses.

Keywords Ambient vibration · Resonance · Modal analysis · Rock mass modulus · Rock arches · Navajo Sandstone

1 Introduction

Measurements of rock mass elastic modulus are scale-dependent (Heuze 1980), complicating efforts to translate laboratory results from core sample testing to scales relevant for most rock engineering problems (Cai et al. 2004). Micro- and macroscopic discontinuities separating intact rock fragments are variably compliant features (Li 2001; Zangerl et al. 2008), making the rock mass deformation (Em) and elastic (Ee) moduli (sensu ISRM 1975) generally well below the Young's modulus obtained from laboratory testing of the corresponding intact rock specimens (Ei) (e.g., Farmer and Kemeny 1992; Wyllie 2003). Accurate prediction of rock mass deformation is crucial in a wide variety of rock engineering applications (e.g., tunnel support, foundations), highlighting the relevance of modulus measurements at engineering-relevant scales.

Different approaches have been proposed to measure or estimate the deformation (Em) and elastic (Ee) moduli of rock masses (ISRM 1979; Palmström and Singh 2001; Cai et al. 2004; Hoek and Diederichs 2006). In situ tests, such as plate jacking, measure stresses and strain over relevant scales (usually by diametrically loading a tunnel or test adit), but are time consuming and expensive to perform, and the results can be strongly affected by excavation damage. A more common approach is to estimate rock mass moduli from empirical relations, often non-linear, developed by comparing in situ test measurements with rock mass classification schemes, e.g., RMR, GSI, and Q (e.g., Bieniawski 1978; Barton 1983; Serafim and Pereira 1983; Hoek et al. 1995; Gokceoglu et al. 2003; Hoek and Diederichs 2006; Shen et al. 2012). In all cases, a high degree of variability is anticipated between the estimated and performance-based rock mass modulus.

Seismic methods represent an alternative means of measuring in situ elastic properties of rock masses. A variety of surface and borehole techniques can be used to measure P- and S-wave velocities over different length scales, and thus

✉ Jeffrey R. Moore
jeff.moore@utah.edu

[1] Department of Geology and Geophysics, University of Utah, Sutton Building, 115 S 1460 E, Room 383, Salt Lake City, UT 84112-0102, USA

Published online: 20 July 2018

calculate the elastic material constants (Barton 2007). However, a large difference in strain amplitudes between static (e.g., plate jacking) and dynamic seismic loads (strains on the order 10^{-3}, 10^{-6}, respectively) gives rise to the common observation that dynamic moduli resolved from field seismic data are typically several times larger than the corresponding static in situ rock mass elastic moduli (Ee and Em) (Lane 1964; Link 1964; Kujundzíc 1979; Stacey 1977; Barton 2007). In general, elastic moduli increase at higher confining pressures with closure of cracks, but can decrease for larger magnitude loading cycles (about the same mean stress) as more discontinuities close (Deere and Miller 1966; Barton 2007).

Here we describe an unconventional experimental method to resolve global rock mass elastic modulus (Ee) from seismic resonance measurements of large freestanding geological features. We present data from five natural arches in Utah formed in Navajo Sandstone, where we have measured resonant modes from ambient seismic data and used these results to calibrate 3D eigenfrequency models. The elastic modulus resolved from this procedure represents the small-strain dynamic behavior of the entire feature, integrating rock mass heterogeneity over large scales to provide a representative value not readily determined from alternative in situ testing procedures.

2 Study Sites and Materials

2.1 Arches

We selected five natural arches of varying dimensions in southern Utah as study sites (Figs. 1, 2). Each arch is formed

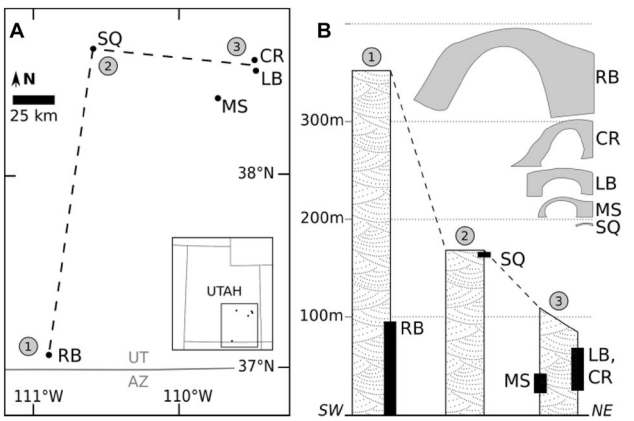

Fig. 1 Geographic and stratigraphic locations of the studied arches. **a** Map of study sites in southern Utah: *SQ* Squint Arch, *RB* Rainbow Bridge, *MS* Mesa Arch, *LB* Longbow Arch, *CR* Corona Arch. **b** Generalized section showing Navajo Sandstone thickness with stratigraphic location of arches. Column numbers correspond with map, Navajo Sandstone thickness is approximated from Blakey et al. (1988). Profile views of arches are at the same scale as the vertical axis

Fig. 2 Arch study sites. **a** Longbow Arch (people on top for scale), **b** Rainbow Bridge (researchers on right side abutment for scale), **c** Corona Arch (person on top for scale), **d** Squint Arch (person underneath for scale), **e** Mesa Arch showing ambient vibration measurement equipment setup, **f** seismometer deployed on Mesa Arch (sensor is approximately 10 cm high)

Table 1 Study sites and resolved elastic modulus from modal analysis

Arch name	Mass (kg)	Location in formation	Elastic modulus, Ee (GPa)
Mesa	2.2 E6	Bottom	5.5
Rainbow	1.0 E8	Bottom	4.7
Corona	1.2 E8	Middle	3.5
Longbow	8.5 E6	Middle	3.4
Squint	8.9 E4	Top	2.0–2.3

Mass refers to the total mass of the arch model assuming a constant density of 2000 kg/m^3. Location is relative within the Navajo Sandstone formation

in Navajo Sandstone; however, the relative location within the formation varies (Table 1). Mesa Arch (38.387968°, − 109.863574°) is located near Moab in Canyonlands National Park. It is ~ 2.5 m thick and ~ 3 m wide and spans 27 m at the edge of a plateau (Starr et al. 2015). Rainbow Bridge (37.077482°, − 110.964153°) is located near the Arizona border in Rainbow Bridge National Monument (Moore et al. 2016). It is among the largest natural arches in world at 75 m high with a span of 83 m. Corona Arch (38.579973°, − 109.620076°) located near Moab, UT, is approximately 33 m high with a span of 34 m and thickness of ~ 7 m. Nearby Longbow Arch (38.542294°, − 109.612790°) is

34 m long and 4 m wide, with a vertical thickness of ~ 8 m. Squint Arch, located in the San Rafael Swell (38.646514°, − 110.673883°), is 12 m long and ~ 2 m wide, with an average thickness of ~ 1 m.

2.2 Navajo Sandstone

Navajo Sandstone is a fine- to medium-grained eolian sandstone of Jurassic age (Nielsen et al. 2009). Large-scale cross-beds are prominent in this massive, cliff-forming unit found extensively throughout Utah, as well as in parts of Idaho, Wyoming and Arizona. It is thickest in southwestern Utah (locally > 600 m), while in the Moab area typical thickness is ~ 100 m (Blakey et al. 1988; Doelling 2010; Fig. 1). Grains are primarily quartz with calcite cement. Variations in iron content give the Navajo Sandstone different coloration facies, which from the top of the formation to the base are: white—iron depleted or 'bleached', pink—mixed bleached and primary red coloration, and brown—iron-enriched sometimes containing iron nodules (Nielsen et al. 2009). Bleaching is most extensive along the flanks of Laramide uplifts, such as the San Rafael Swell where Squint Arch is located (Beitler et al. 2003). Iron content also affects the mechanical properties of the material, with iron-rich Navajo Sandstone being slightly denser, stronger and less friable. Exposed surfaces often have degraded mechanical properties in the outermost centimeters from meteoric leaching of calcite (Dames & Moore 1972).

Mechanical properties of Navajo Sandstone vary with depositional environment, diagenetic alternation, and weathering. However, in general, the sandstone has average porosity in the range of 20–30% (Schultz et al. 2010), and bulk density of approximately 2000 kg/m^3 (Dames & Moore 1972; new measurements in this study). Uniaxial compressive strength can vary markedly across the formation from 27 MPa (this study) to ~ 40 MPa (Dames & Moore 1972) to > 200 MPa (Goodman 1989) in conjunction with differences in iron content. Published laboratory data also show variations in elastic (Young's, tangent) modulus (Ei): Dames & Moore (1972) tested core samples taken from loose blocks at the base of Rainbow Bridge and found Ei = 10 GPa, while core samples from the Glen Canyon Dam site ~ 50 km distant had Ei = 15 GPa (Deere and Miller 1966). The latter specimens were found to have lower Young's modulus on the initial loading cycle of Ei = ~ 10 GPa (Santi et al. 2000). New testing in this study (following ISRM 1979 procedures) of four core samples taken from a loose block of Navajo sandstone collected near Corona and Longbow arches found Ei = 13.7 ± 1.5 GPa.

3 Methods

3.1 Seismic Resonance Data

We extract information on the resonant frequencies of freestanding natural arches from ambient vibration data (Starr et al. 2015; Moore et al. 2016). We use three-component Nanometrics Trillium Compact seismometers (flat frequency response between 0.05 and 100 Hz) with 24-bit Centaur data loggers recording continuous data at 100–200 Hz. We place at least one sensor on the feature being assessed and another ~ 100 m away on flat, solid bedrock for reference. This allows us to isolate signals of interest related to resonance of the arch. In some cases, we deploy multiple seismometers on the arch, which provides additional data useful for resolving resonant modes. All sensors are simply placed on bare bedrock (not permanently affixed), leveled and aligned to north. They are covered to minimize direct exposure to wind and solar radiation.

We process ambient vibration data for spectral content and polarization attributes following methods described by Koper and Hawley (2010). Details of the processing are reported by Starr et al. (2015) and Moore et al. (2016). Example ambient vibration spectra from Rainbow Bridge are shown in Fig. 3, where we compare power spectral density plots from on the bridge to those from the bedrock canyon floor. We observe strong spectral peaks at frequencies between 1 and 10 Hz on the bridge that are not found on the reference sensor, which we interpret as resonant frequencies of Rainbow Bridge. The peak at ~ 0.18 Hz is the 'microseism' created by ocean-generated seismic noise (Longuet-Higgins 1950), and is measured equally on both sensors.

3.2 Modal Analysis

We retrieve polarization attributes (azimuth and dip of particle motion) from field data at the identified resonant frequencies. The results provide experimental constraints on the modal displacement vector at the location of the seismometer. For example, for the fundamental resonant mode of Rainbow Bridge identified at 1.1 Hz (Fig. 3), we find that ground motion at the sensor location is oriented perpendicular to the trend of the bridge and is predominantly horizontal. Modal vectors for the first eight modes of vibration for Rainbow Bridge are shown on inset stereo plots in Fig. 5. Experimental data for each identified resonant mode thus consist of frequency and vector orientation at the sensor location. These are then used to calibrate the following numerical modal analyses.

Numerical modal analysis allows us to confirm experimental results and resolve the full displacement field for

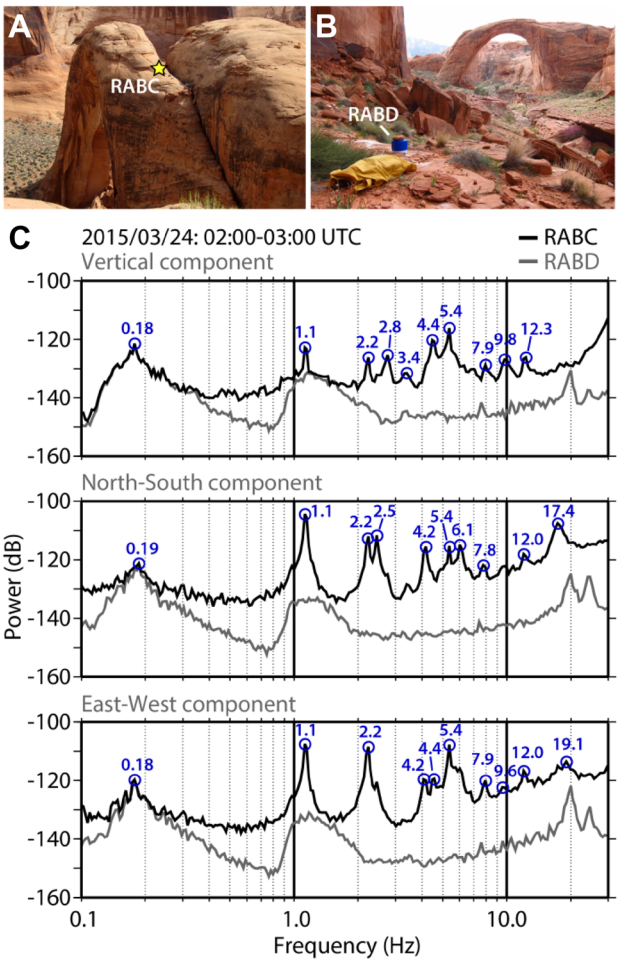

Fig. 3 Ambient vibration data. **a** Rainbow Bridge showing location of sensor RABC on the span; **b** reference sensor RABD on the canyon floor. **c** Power spectral density plots for both sensors for a typical 1-h time block. Peaks in power indicate resonant frequencies of the bridge

each resonant mode. We perform three-dimensional eigenfrequency analysis using the finite-element software COMSOL Multiphysics (http://www.comsol.com). Required input parameters are: geometry of the arch, mechanical boundary conditions, and material properties. To develop geometrical models, we use ground- and drone-based photogrammetry (see Moore et al. 2016). In cases where photographic coverage is sub-optimal (e.g., Mesa Arch), we create basic geometrical models from field measurements. Mechanical boundary conditions are determined from field assessment; in general, the task is determining which boundaries will be fixed in modal analysis (i.e., places where the arch is adhered to adjoining bedrock). A geometrical model of Rainbow Bridge created from ground-based photogrammetry is shown in Fig. 4, also showing boundaries we selected to be held fixed in modal analysis.

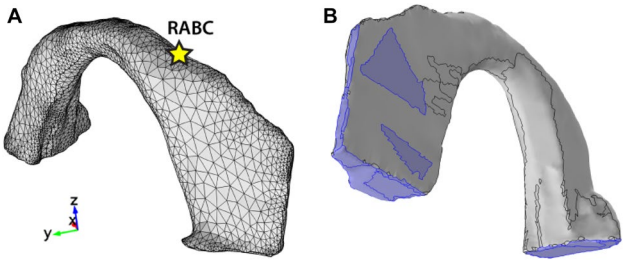

Fig. 4 3D model of Rainbow Bridge. **a** Geometry derived from ground-based photogrammetry showing finite-element mesh and location of sensor RABC. **b** Blue faces are held fixed in numerical modal analysis, simulating areas where the bridge is adhered to adjoining bedrock

Material properties are varied in numerical analyses to achieve best match with field data. Two material properties affect the resonant frequencies: density and elastic moduli. We hold the former constant, assuming a common value for Navajo Sandstone of 2000 kg/m^3 (Dames & Moore 1972 and our new measurements), and then vary elastic modulus to achieve best match between measured and modeled frequencies. In addition to matching frequencies, we test for correspondence between measured and predicted modal vectors at the seismometer location(s). Example results for Rainbow Bridge are displayed in Fig. 5. Model results compare well with measured data for seven of the first eight modes, matching vibrational frequencies and polarization orientations generally within 10%, and indicating our model is appropriately parameterized.

4 Results

Our analysis results in an experimentally determined, numerically calibrated, globally representative estimate of rock mass elastic modulus (Ee). At Mesa Arch, we were able to match field and numerical results for the first four modes of vibration and resolve Ee = 5.5 GPa (Table 1). At Rainbow Bridge, we matched seven of the first eight modes of vibration implementing Ee = 4.7 GPa. At Corona Arch, we matched four of the first six modes of vibration determining Ee = 3.5 GPa, while at Longbow Arch we matched three modes of vibration and resolved Ee = 3.4 GPa. Results for Squint Arch were less optimal; we were only able to match the fundamental frequency of vibration finding Ee = 2.0–2.3 GPa. These values are all of the same order of magnitude and relatively similar (variation of ±45% from the mean), as expected for features formed in the same material (Navajo Sandstone). However, significant and systematic differences occur that cannot be attributed to inaccuracies on our field data or numerical models.

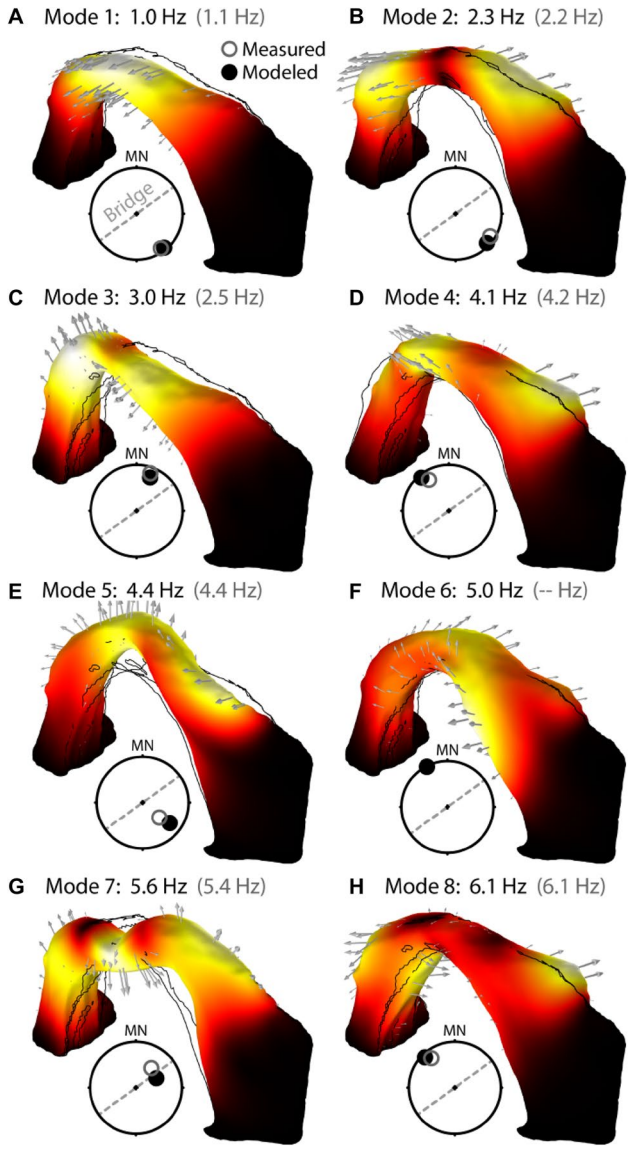

Fig. 5 Modal analysis of Rainbow Bridge. **a**–**h** First eight-modeled modes of vibration with accompanying eigenfrequency listed; measured values shown in parentheses (see Fig. 3). Color map, deformed body, and arrows illustrate deformation at zero phase (normalized relative scale for each mode), wireframe shows static form. Stereo plots compare measured (open circles) and modeled (filled circles) polarization vectors; trend of Rainbow Bridge indicated by the dashed line. *MN* Magnetic north

In Table 1, we compare modulus estimates for each arch with the scale of the feature (given as total mass of the arch), as well as its relative position within the Navajo Sandstone formation. A size effect might be expected due to the increased likelihood of intersecting discontinuities at larger scales, while differences in iron content within the Navajo could give rise to systematic variations in modulus from the top to the bottom of the formation. Our results reveal no significant trends in scale; however, we find that the elastic modulus for arches formed in the lower Navajo Sandstone is ~50% greater than those from the middle of the formation, and ~2.5 times greater than that from the top of the formation. These differences likely arise from increased iron content in the lower Navajo, which helps cement sand grains making the material stiffer. Iron nodules are abundant at Rainbow Bridge providing evidence of enriched iron content.

5 Discussion

Our experimental procedure uses ambient vibration field data to calibrate 3D numerical models, simulating the vibrational modes of freestanding geological features such as arches. After implementing accurate geometry, two material properties can be varied in the model to match resonant frequencies, density (ρ) and elastic modulus (Ee). Resonant frequencies (f) are a function of these parameters as:

$$f \propto \sqrt{(\mathrm{Ee}/\rho)}. \quad (1)$$

Assuming a typical density for Navajo Sandstone of 2000 kg/m^3 (and holding this value constant for all analyzed features) allows us to vary Ee to achieve best match with measured resonant frequencies. Correctly matching the values, as well as the distribution of values, for several consecutive resonant frequencies lends confidence to our results. Moreover, correctly reproducing polarization vectors indicates that model geometry and boundary conditions are appropriate. The elastic modulus thus determined incorporates heterogeneity over the scale of the arch (Table 1), providing a unique and valuable measure of rock mass modulus not easily obtained by other experimental means. For comparison, Palmström and Singh (2001) noted for massive rock that Em can be approximated as 0.5 Ei. Our resolved values of modulus (Table 1) compare relatively well with this simple formulation, especially at Rainbow Bridge where we have accompanying measurements of Ei.

We assume uniform material properties for arches analyzed in this study. Although this represents a simplification of the true rock mass structure, the generally good match between measurements and model results indicates that approach is suitable for describing the global properties of these features. Alternatively, the degree of match between measurements and model may provide insight into material heterogeneity, or lack thereof. For example, at Rainbow Bridge, assuming uniform material properties, we were able to match seven modes of vibration. Applying the same assumption at Squint Arch, on the other hand, we were only able to match 1–2 modes. Squint Arch lies at the top of the Navajo Formation and the rock mass is cross-bedded and strongly leached. We hypothesize that material anisotropy may be more pronounced because of this leaching and contribute to differences between measurements and model results. Rainbow Bridge also contains bedding,

cross-beds and other anisotropic features, but the global elastic modulus appears to be approximately isotropic.

It is feasible to let density vary in our analysis, but we opted to retain a constant value for all features formed in the same material. We note that the density of Navajo Sandstone is expected to vary between ~2000 and 2200 kg/m^3 (Dames & Moore 1972 and new measurements here), which is a range of only 10%. Elastic modulus, on the other hand, is likely to vary over a larger range; e.g., limited laboratory data show 50% variation of Ei. Our resolved values of rock mass elastic modulus similarly show variations of up to ~100%, much larger than possible variations in bulk density. Implementing rock mass structural compartments with varying mechanical properties would also be feasible in our numerical analysis; however, without detailed structural mapping or geophysical investigation these are likely to be poorly characterized. Satisfactory match between our field data and models suggests that structural zonation is not necessary to describe the global vibrational properties of the arches studied in this work.

While our method provides a non-destructive and non-invasive means of evaluating large-scale elastic properties of a rock mass, it has notable limitations. For example, we require in situ measurement of ambient vibration, meaning a seismometer usually has to be placed on top of the feature being assessed, which is not always feasible. Furthermore, accessibility often limits the location where we can measure ambient vibrations, even when the top of the feature can be reached. This can affect our ability to resolve vibrational modes; for example, if our sensor is located on a nodal point for a particular mode (the point of zero displacement), the mode would not be observed.

The modulus we determine describes the global, small-strain elastic properties of the investigated feature. It is important to place our results within the range of strains used to differentiate dynamic and static measurements (~10^{-3} and ~10^{-6}, respectively; Barton 2007). Analyzing representative ambient vibration data from Mesa Arch, we measure typical peak displacements (out-of-plane horizontal) of ~1 µm. Translating these into longitudinal strain (using formulations for bending of a prismatic beam), we estimate the order of peak dynamic strains represented by our data to be approximately 10^{-8}. Thus, while strains in this study resemble dynamic measurements (i.e., controlled source seismic), the elastic moduli resolved are more closely related to static measurements, being smaller than the corresponding laboratory data. No complementary in situ seismic velocity measurements are available at these sites to further explore this observation. While our technique is small-strain, akin to dynamic measurements, the resonant deformations we measure still likely involve some compliant opening and closing of rock mass discontinuities at multiple scales, potentially explaining why our resolved Ee more closely aligns with expected static in situ values.

Mechanical boundary conditions represent arguably the largest unknown in our models, and therefore introduce a significant source of uncertainty for the determined elastic modulus. First, we select the faces of the arch that are to be held fixed in modal analysis (e.g., Fig. 4). In some cases, this is clear, but in others the fixed areas are obscured (e.g., a deep crack open at the surface and closed at the base), and must be characterized from field assessment. Moreover, we must determine the appropriate total scale of the vibrating feature, i.e., the model extents that include all mass participating in each vibrational mode. In the cases analyzed here, this was relatively straightforward, and errors only arose if the models were cropped too tightly (demonstrated in Fig. 6). Adding additional mass in the models (e.g., extending the abutments) had little effect on our results since this

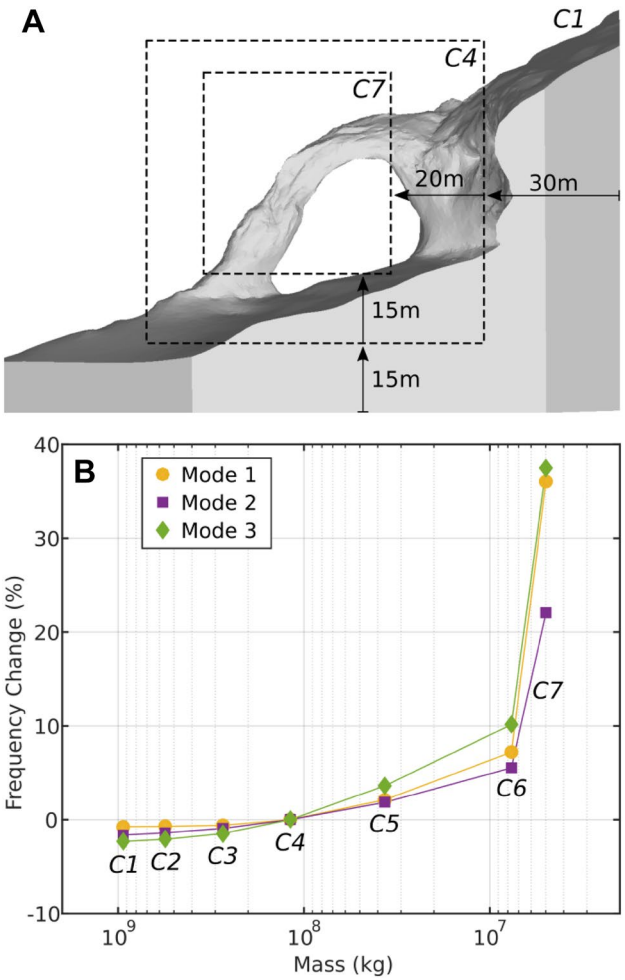

Fig. 6 Sensitivity of modal analysis results to boundary conditions at Corona Arch using seven incrementally cropped 3D models (C1–C7). **a** Geometry comparison between cropped models C1, C4, and C7. Labeled distances indicate relative cropping for each model, with dashed lines outlining the cropped model boundaries. **b** Frequency changes for the first three modes of vibration, normalized to best fitting model C4 and plotted against total model mass

mass was generally immobile, while in testing at other study sites not described here, we have allowed the arch to be situated within a larger topography and found the modeled modes of vibration unaffected. At other locations, however, the position of fixed boundaries can be unclear, such as arches formed within larger freestanding features such as fins. We gain confidence in our model boundary conditions when we are able to match frequencies and polarization vectors for a number of sequential modes.

Past measurements at Mesa Arch (Starr et al. 2015) have shown that resonant frequencies are non-stationary, varying by several percent throughout the day and year in direct correspondence with rock temperature (see also Bottelin et al. 2013). This observation indicates that elastic modulus is, in turn, variable over short- and long-time scales; measured frequency variations by Starr et al. (2015) amount to a ~6% daily change in Ee. Such changes likely reflect stiffening cycles in the rock mass facilitated by crack closure accompanying thermal expansion and increased axial stress. Short-term temperatures only reach shallow depths in rock (tens of cm), indicating that this stiffening occurs only within a thin skin of the arch, while longer term (e.g., yearly) thermal cycles heat the full thickness. While such changes appear to be fully reversible (i.e., recoverable with no permanent change), frequency monitoring over time can equally be used to discern permanent change or damage to natural geological landforms and civil structures (e.g., Clinton et al. 2006; Lévy et al. 2010; Bottelin et al. 2017; Burjánek et al. 2018).

6 Conclusions

We describe a new experimental protocol to derive a globally representative rock mass elastic modulus (Ee) from ambient vibration measurements on freestanding rock landforms. The field methodology is simple and non-invasive, which is ideal for evaluating material properties of culturally significant or fragile geologic features. We determined the elastic modulus of five natural arches in southern Utah, each formed in Navajo Sandstone. Estimated Ee ranges from 2.0 to 5.5 GPa, values which are roughly 20–50% of the intact rock modulus (Ei) measured from laboratory testing. Variations across the studied features are significant (i.e. not explained by error or uncertainty), and are most likely related to differing amounts of iron content correlated with stratigraphic position. We study rock arches in particular, but the technique is equally suitable for assessing other natural and man-made features. Complications arise in the case of uncertain mechanical boundary conditions implemented in numerical modal analyses or strong material anisotropy. We propose the approach offers a useful method for in situ assessment of rock mass elastic modulus for fragile freestanding landforms, an important material property not easily determined from field testing.

Acknowledgements We thank the following tribal organizations for allowing access to Rainbow Bridge: Navajo Nation, Hopi Tribe, Kiabab Paiute Tribe, San Juan Southern Paiute Tribe, White Mesa Ute, and the Pueblo of Zuni. We gratefully acknowledge the University of Utah Center for High Performance Computing for providing computational resources. This study was funded by the National Science Foundation Grant EAR-1424896 to Moore and Thorne.

References

Barton N (1983) Application of Q-system and index tests to estimate shear strength and deformability of rock masses. Proc. Int. Symp. on Engineering Geology and Underground Constructions, pp 51–70

Barton N (2007) Rock quality, seismic velocity, attenuation and anisotropy. CRC Press, London

Beitler B, Chan MA, Parry WT (2003) Bleaching of Jurassic Navajo sandstone on Colorado Plateau Laramide highs: evidence of exhumed hydrocarbon supergiants? Geology 31(12):1041–1044

Bieniawski ZT (1978) Determining rock mass deformability: experience from case histories. Int J Rock Mech Mining Sci Geomech Abstr 15(5):237–247

Blakey RC, Peterson F, Kocurek G (1988) Synthesis of late Paleozoic and Mesozoic eolian deposits of the Western Interior of the United States. Sed Geol 56:3–125

Bottelin P, Lévy C, Baillet L, Jongmans D, Guéguen P (2013) Modal and thermal analysis of Les Arches unstable rock column (Vercors massif, French Alps). Geophys J Int 194:849–858. https://doi.org/10.1093/gji/ggt046

Bottelin P, Baillet L, Larose E, Jongmans D, Hantz D, Brenguier O, Cadet H, Helmstetter A (2017) Monitoring rock reinforcement works with ambient vibrations: La Bourne case study (Vercors, France). Eng Geol 226:136–145

Burjánek J, Gischig V, Moore JR, Fäh D (2018) Ambient vibration characterization and monitoring of a rock slope close to collapse. Geophys J Int 212(1):297–310

Cai M, Kaiser PK, Uno H, Tasaka Y, Minami M (2004) Estimation of rock mass deformation modulus and strength of jointed hard rock masses using the GSI system. Int J Rock Mech Min Sci 41(1):3–19

Clinton JF, Case Bradford S, Heaton TH, Favela J (2006) The observed wander of the natural frequencies in a structure. Bull Seismol Soc Am 96(1):237–257

Dames & Moore (1972) Geological and structural evaluation of Rainbow Bridge, Rainbow Bridge National Monument, Utah, Unpublished consultant's report to the Upper Colorado River Commission, Salt Lake City

Deere DU, Miller RP (1966) Engineering classification and index properties for intact rock. Technical report AFWL-TR-65-116 for the Air Force Weapons Laboratory, NM

Doelling HH (2010) Geology of Arches National Park, Utah. In: DA Sprinkel, TC Chidsey, PB Anderson (eds) Geology of Utah's Parks and Monuments, vol 28. Utah Geological Association Publication, Salt Lake City, pp 11–36

Farmer IW, Kemeny JM (1992) Deficiencies in rock test data. Proc. Int. Conf. Eurock '92, Thomas Telford, London, pp 298–303

Gokceoglu C, Sonmez H, Kayabasi A (2003) Predicting the deformation moduli of rock masses. Int J Rock Mech Min Sci 40(5):701–710

Goodman RE (1989) Introduction to rock mechanics. Wiley, New York

Heuze FE (1980) Scale effects in the determination of rock mass strength and deformability. Rock Mech 12(3–4):167–192
Hoek E, Diederichs MS (2006) Empirical estimation of rock mass modulus. Int J Rock Mech Min Sci 43(2):203–215
Hoek E, Kaiser PK, Bawden WF (1995) Support of underground excavations in hard rock. A.A. Balkema, Rotterdam
ISRM (1975) Commission on terminology, symbols and graphic representation. International Society for Rock Mechanics (ISRM), Salzburg
ISRM (1979) Suggested methods for determining in situ deformability of rock. Int J Rock Mech Min Sci Geomech Abstr 16:195–214
Koper KD, Hawley VL (2010) Frequency dependent polarization analysis of ambient seismic noise recorded at a broadband seismometer in the central United States. Earthq Sci 23:439–447. https://doi.org/10.1007/s11589-010-0743-5
Kujundzíc B (1979) Use of tests and monitoring in the design and construction of rock structures, vol 3. Proc. of 4th Int. Congr. Rock Mech. (ISRM), Montreux. Balkema, Rotterdam, pp 181–186
Lane RGT (1964) Rock foundations. Diagnosis of mechanical properties and treatment, vol 1. Proc. 8th Int. Congress on Large Dams, Edinburgh. ICOLD, Paris, pp 141–165
Lévy C, Baillet L, Jongmans D, Mourot P, Hantz D (2010) Dynamic response of the Chamousset rock column (Western Alps, France). J Geophys Res 115:F04043. https://doi.org/10.1029/2009JF001606
Li C (2001) A method for graphically presenting the deformation modulus of jointed rock masses. Rock Mech Rock Eng 34(1):67–75
Link H (1964) Evaluation of elasticity moduli of dam foundation rock determined seismically in comparison to those arrived at statically, vol 1. Proc. 8th Int. Congress on Large Dams, Edinburgh. ICOLD, Paris, pp 833–858
Longuet-Higgins MS (1950) A theory of the origin of microseisms. Philos Trans R Soc Lond Ser A Math Phys Sci 243:1–35
Moore JR, Thorne MS, Koper KD, Wood JR, Goddard K, Burlacu R, Doyle S, Stanfield E, White B (2016) Anthropogenic sources stimulate resonance of a natural rock bridge. Geophys Res Lett 43:9669–9676. https://doi.org/10.1002/2016GL070088
Nielsen G, Chan MA, Petersen EU (2009) Diagenetic coloration facies and alteration history of the Jurassic Navajo Sandstone, Zion National Park and vicinity, southwestern Utah. In: Tripp BT, Krahulec K, Jordan JL (eds) Geology and geological resources and issues of Western Utah. Utah Geological Association Publication 38, Salt Lake City, pp 67–96
Palmström A, Singh R (2001) The deformation modulus of rock masses—comparisons between in situ tests and indirect estimates. Tunn Undergr Space Technol 16(2):115–131
Santi PM, Holschen JE, Stephenson RW (2000) Improving elastic modulus measurements for rock based on geology. Environ Eng Geosci 6(4):333–346
Schultz RA, Okubo CH, Fossen H (2010) Porosity and grain size controls on compaction band formation in Jurassic Navajo Sandstone. Geophys Res Lett 37:L22306. https://doi.org/10.1029/2010GL044909
Serafim JL, Pereira JP (1983) Consideration of the geomechanics classification of Bieniawski. Proc. Int. Symp. on engineering geology and underground constructions, pp 1133–1144
Shen J, Karakus M, Xu C (2012) A comparative study for empirical equations in estimating deformation modulus of rock masses. Tunn Undergr Space Technol 32:245–250
Stacey TR (1977) Seismic assessment of rock masses, vol 2. Proc. symposium on exploration for rock engineering. Johannesburg, pp 113–117
Starr AM, Moore JR, Thorne MS (2015) Ambient resonance of Mesa Arch, Canyonlands National Park, Utah. Geophys Res Lett. https://doi.org/10.1002/2015GL064917
Wyllie DC (2003) Foundations on rock: engineering practice. CRC Press, London
Zangerl C, Evans KF, Eberhardt E, Loew S (2008) Normal stiffness of fractures in granitic rock: a compilation of laboratory and in situ experiments. Int J Rock Mech Min Sci 8:1500–1507